ANNALS OF GEOPHYSICS, 68, 6, S685, 2025; doi:10.4401/ag-9290
OPEN ACCESS

Exploring Earthquake Depth variability through Between-Event Residuals: Insights from Italy

Claudia Mascandola[*,1], Francesca Pacor[1], Giovanni Lanzano[1], Fadel Ramadan[1], Paola Traversa[2]

(1) Istituto Nazionale di Geofisica e Vulcanologia (INGV), Milan, Italy
(2) Électricité de France (EDF), DIPNN-DI-TEGG, Aix-en-Provence, France

Article history: received February 02, 2025; accepted September 19, 2025

Abstract

Despite the crucial importance of accurate event localizations, focal depths are generally poorly constrained, especially for very shallow events (depth <10 km), which are often mislocated. In this study, we investigate whether the event-specific ground-motion residuals, δB_e, are correlated with focal depth. In particular, we examine whether and to what extent the focal depth influences the spectral shape of the δB_e curves.

The residual investigated in this study are derived from the ITACAext 1.0 flatfile, which is related to the ITalian ACcelerometric Archive (i.e., ITACA database) and collects waveforms of seismic events with magnitude greater than 3.0, recorded in Italy since 1972. The residual analysis is conducted using the latest predictive ground-motion model for shallow crustal earthquakes in Italy as a reference. To emphasize the δB_e differences for events with varying focal depths, the attenuation in the ground-motion model is measured using the Joyner-Boore distance.

A cluster analysis is applied on the δB_e spectral curves, revealing systematic trends that can be related to different focal depths. In particular, a cluster of very shallow earthquakes (<10 km; VSE) is identified. This cluster is characterized by δB_e amplitudes that are systematically positive at long periods (>1 s) and negative at short periods (<1 s). Opposite features are observed for deeper earthquakes (>10 km), with δB_e amplitudes that are systematically negative at long periods (>1 s) and positive at short periods (<1 s). As expected, the overall δB_e amplitudes of deep events decrease as depth increases.

The proposed method appears to be a promising tool for identifying mislocated events or detecting earthquakes erroneously classified as shallow crustal seismicity (i.e., very shallow earthquakes of volcanic origin or deep earthquakes in subduction areas). Improving the estimates of focal depths would lead to a reduction in the variability of the ground motion models in epicentral area, with significant implications on hazard estimates.

Keywords: Earthquake ground motions; Focal depth; Very shallow events; Earthquake source observations; Wave propagation

1. Introduction

The spatial and temporal distribution of earthquakes is a crucial factor in seismic hazard assessment. It plays a key role in developing seismotectonic and recurrence models, defining ground motion models, and identifying the most significant scenarios for seismic and tsunami risk assessment. Despite its crucial importance, earthquake depth is determined with less accuracy than the geographic coordinates of the epicenter. Several factors can lead to low hypocentral location accuracy, such as insufficient station coverage or poor seismological network geometry, inaccuracy and errors in time arrival picking of seismic phases, modeling errors and velocity model uncertainties (e.g., Gomberg et al., 1990; Jansky et al., 2009; Spallarossa et al., 2001; Latorre et al., 2023).

The impact of these issues on earthquake depth estimation is particularly critical for Very Shallow Events (depth <10 km; VSE), whereas deeper events are less vulnerable to these problems (Janský et al., 2009). This point is illustrated in Fig. 1, where we compare revised hypocentral depths (from CAT3 catalog in Chiaraluce et al., 2022) of about 500 events in Central Italy, with those provided by the control room of Istituto Nazionale di Geofisica e Vulcanologia (INGV, see Data Availability) that provides near-real-time automatic locations, manually reviewed by expert analysts soon after the origin time of the earthquake (Margheriti et al., 2021). It can be observed that the depth estimates provided by the INGV control room leads to a systematic overestimation of the VSE depth with respect to relocated values (Fig. 1).

In principle, event relocation should correct biases in hypocentral depth, but this is not systematically applied and, even for relocated events, not all uncertainties can be effectively reduced, thus biases can still persist (Margheriti et al., 2021). In particular, the hypocenters of the INGV bulletin (Italian Seismological Instrumental and parametric Data-base, ISIDe, ISIDe Working Group, 2007) are obtained using a very simple velocity model, consisting of two main layers and a half-space with a constant V_P and V_P/V_S ratio (Menichelli et al., 2022). This simplified model leads to a clustering of the bulletin earthquake locations around 11 km, corresponding to the boundary between the upper and lower crust (Menichelli et al., 2022), which is likely an effect of the strong velocity contrast between the two model layers.

It is well known that large uncertainties on focal depths may seriously affect not only the definition of seismotectonic models, based on correct assignment of the events to the corresponding fault system (e.g., Eva et al., 2020; Michele et al., 2020; Karakostas et al., 2021; Barchi et al., 2021), but also the identification of induced earthquakes (e.g., Atkinson et al., 2016; Caciagli et al., 2015; Peruzza et al., 2021), the estimation of spectral parameters (e.g., Pacor et al., 2016; Castro et al., 2021; Bindi et al., 2021, 2023a, 2023b), and the prediction of ground-motion models (GMMs), especially in near-source regions, where the shaking is characterized by very high

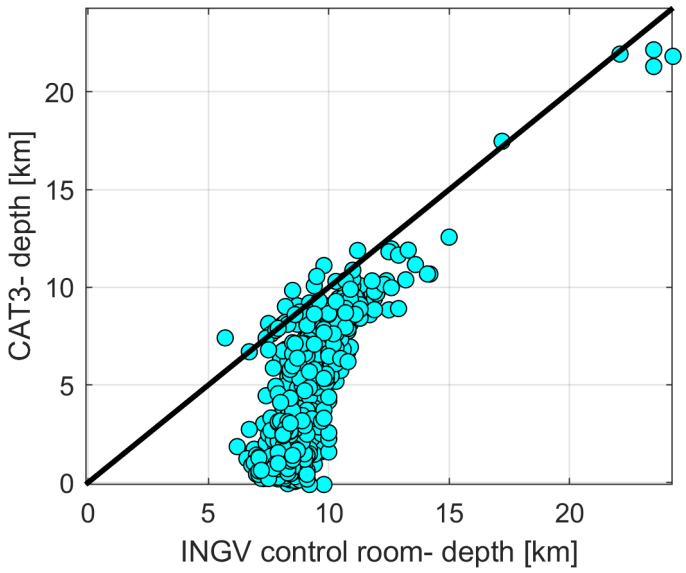

Figure 1. Comparison between relocated hypocentral depths of 561 events, related to the 2016-2017 Central Italy seismic sequence (CAT3 catalog in Chiaraluce et al., 2022), and the corresponding ones provided by INGV control room (see Data Availability).

variability (e.g., Atkinson et al., 2016; Kotha et al., 2020; Parker et al., 2022). In this regard, considering the known impact of focal depth on seismic ground motion, errors in hypocentral depth should systematically affect the comparison between observed and predicted ground motions. Systematic deviations from a reference ground-motion model are quantified through residual analysis, defined as the difference between observed ground motions and model predictions. Residual analysis of ground-motion data is a standard practice in seismology that has been applied for many purposes, such as bias identification on co-located sensors (e.g., Lanzano et al., 2025), consistency check of a dataset (e.g., Bindi et al., 2019; Traversa et al., 2020; Mascandola et al., 2022), site- and event-specific corrections (e.g., Bindi et al., 2011), development of non-ergodic models (e.g., Sgobba et al., 2021b), and probabilistic seismic hazard assessments (e.g., Liou and Abrahamson, 2024). In particular, the residual decomposition allows for the identification of systematic errors associated with the event, propagation path, and site response (e.g., Al Atik et al., 2010; Bindi et al., 2011).

In this study, we focus on the event component to identify anomalous trends and interpret them in relation to earthquake depths reported in seismic catalogs. The residual analysis is performed at the Italian scale using data from the ITACAext flatfile (version 1.0, Brunelli et al., 2022). The residuals are computed on both the horizontal and vertical ground motion components, considering the ITA18 model (Lanzano et al., 2019) as reference for the horizontal components, and the Ramadan et al. (2021) vertical-to-horizontal ratios as reference for the vertical components. However, as the residual analysis of the vertical ground-motion components produced results comparable to those of the horizontal ones, only the latter are presented and discussed.

Finally, a cluster analysis is performed on the residual spectral curves to group events that show similar systematic biases and identify possible dependencies on earthquake features, such as tectonic regime and focal depth. The outcomes are verified on a high-quality seismic catalog of relocated events in Central Italy (Chiaraluce et al., 2022).

2. Dataset

The dataset used is the ITACAext flatfile (version 1.0; Brunelli et al., 2022), a parametric table created to disseminate intensity measures and metadata relative to the ITACA database (Italian Accelerometric Archive; Russo et al., 2022), the most complete archive of moderate-to-severe earthquake records collected in Italy since 1972. In particular, ITACAext refers to version 3.2 of ITACA, which includes manually processed data up to December 31st 2020. It provides 36 ordinates of the response spectra (SA) in the period interval 0.01-10 s. To obtain more robust estimates of the residual terms, ITACAext is enriched with records not stored in the ITACA database. In particular, ITACAext includes some strong-motion data acquired by seismic networks of neighboring countries (e.g., France, Switzerland, Slovenia, Albania and Montenegro), as well as M<4 data recorded by broad-band sensors of the National Seismic Network (RSN), available from the EIDA data stream (Strollo et al., 2021; see Data and Resources) in low seismicity or poorly monitored areas.

Overall, the study dataset is composed of 41,109 waveforms from 1,973 events and 1,967 stations. Most of the events span from M_W 3.0 to 5.0, with distances (Joyner and Boore, R_{JB}, or epicentral distances, R_{epi}) between 10 and 200 km (Fig. 2a), and hypocentral depths around 10 km (Fig. 2b). The magnitude estimates are homogenized into moment magnitude (M_W) from the RCMT (Regional Centroid Moment Tensor; Pondrelli et al., 2002) method. The hypocentral location of the Italian events is provided by the INGV surveillance service (see Data Availability), which provides near-real-time automatic locations, manually reviewed by expert analysts soon after the origin time of the earthquake (Margheriti et al., 2021). The hypocentral location of the events in neighboring countries comes from the European-Mediterranean Seismological Centre (EMSC-CSEM; see Data Availability) or from the Bulletin of International Seismological Centre (ISC; see Data Availability). Since neither the hypocentral locations of the Italian events nor those of the neighboring countries are relocated, the focal depths of the ITACAext flatfile may be biased, especially on the VSE. For the purpose of this study, we exclude only records with epicentral distance greater than 250 km, while no filter is applied on hypocentral depth and on the tectonic regime, thus including also volcanic and subduction events to investigate the behavior of the corresponding residuals.

The spatial distribution of the events of the ITACAext dataset is reported in Fig. 3: those with focal depth lower than 10 km are quite homogeneously distributed along the active tectonic structures of the Apennines and the Alps (Fig. 3a). Events with depth between 10 and 30 km show a similar distribution, even if a reduced number of earthquakes is observed in Central Italy, with an increase both in the Northern and Southern Apennines (Fig. 3b).

The deep events between 30 and 80 km are located in Southern Italy, near the Gargano Promontory, or along the outermost front of the Northern Apennines (Fig. 3c). Finally, the deepest events (more than 80 km depth) are all located in Southern Italy, within the Tyrrhenian subduction zone (Fig. 3d).

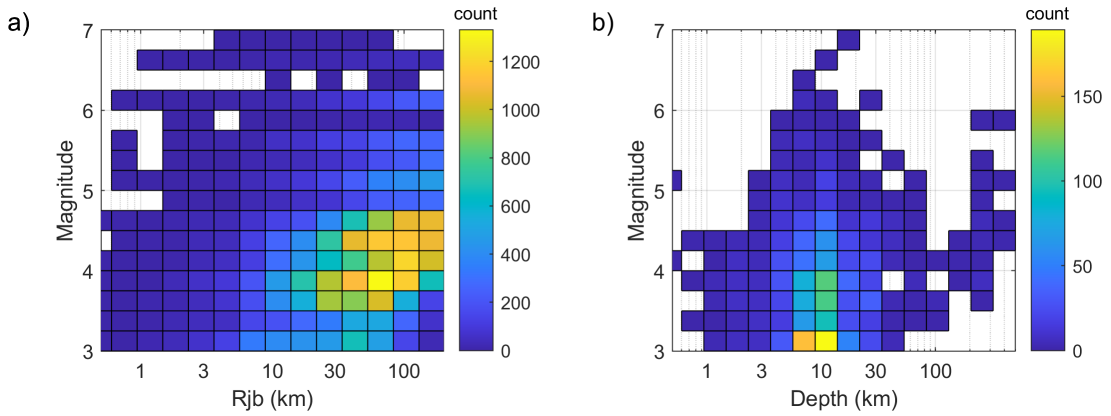

Figure 2. (a) Magnitude-distance (Joyner-Boore/epicentral distance, R) and (b) magnitude-depth distributions for the ITACAext dataset.

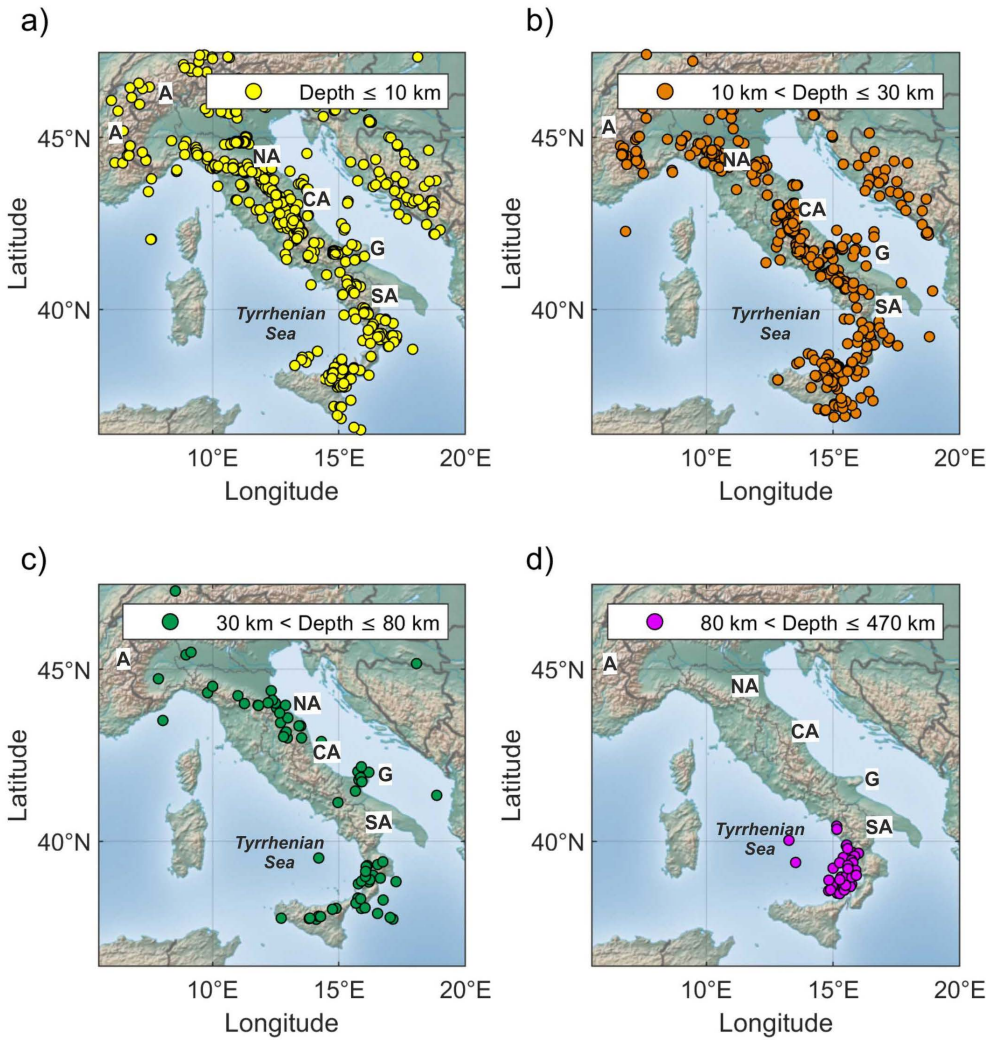

Figure 3. Maps of earthquakes in the ITACAext flatfile, colored according to depth intervals. A: Alps; NA: Northern Apennines; CA: Central Apennines; SA: Southern Apennines; G: Gargano Promontory.

3. Method

To investigate the systematic errors associated with an individual earthquake, the total residuals (R_{es}) are computed as the difference between the natural logarithm of observations, $\ln(oss)$, and the natural logarithm of predictions, $\ln(pred)$, for both the horizontal and vertical ground motion components.

The observations are those reported on the ITACAext flatfile, whereas the predictions are those obtained with the latest ground-motion model for Italy. Specifically, we consider the partially non-ergodic ground motion model ITA18 (Lanzano et al., 2019) as a reference model for horizontal components. The residual analysis on the vertical components is performed using the ITA18_VH model developed by Ramadan et al. (2021) for vertical-to-horizontal (VH) response spectral ratio, consistent with the ITA18 model for horizontal ground motion. The residual analysis is carried out on the ordinates of the acceleration response spectra, at 5% damping, in the 0.01 to 5 s period range.

To highlight the biases associated with focal depth, some working hypotheses are adopted:

1) ITACAext flatfile is used considering events of different tectonic regime (i.e., shallow crustal, volcanic and subduction earthquakes);
2) the Joyner-Boore distance, R_{JB} (Joyner and Boore, 1981; the closest distance to the rupture projection on the surface) or the epicentral distance R_{epi}, is adopted as distance metric in ITA18 model, to emphasize the bias on the hypocentral depth.

The simplest residual decomposition is performed by decomposing the total residuals according to the following expression (see Al-Atik et al., 2010, for an excursus on terminology):

$$R_{es} = \ln(oss) - \ln(pred) = a_0 + \delta B_e + \delta W_{es} \tag{1}$$

where the subscripts e and s refer to event and station, respectively. a_0 is the median offset, δB_e is the between-event term, i.e. the median residual for each event with respect to model prediction, and δW_{es} is the within event, i.e. the leftover aleatory residual. The residuals are decomposed using the mixed effects regression (Bates et al., 2014), usually adopted for the calibration of non-ergodic ground motion models. The δB_e residuals are characterized by zero-mean and standard deviation τ. Similarly, δW_{es} residuals are zero-mean with standard deviation Φ. The total standard deviation σ, related to the total residual, R_{es}, can be computed as:

$$\sigma = \sqrt{\tau^2 + \Phi^2} \tag{2}$$

In this study, we focus on the between-event terms, δB_e, as these represent all the event-specific effects not included in the GMM functional form. Indeed, the predictor variables of the ITA18 model are the moment magnitude M_W, the source-to-site distance R, the style of faulting, and the $V_{S,30}$ as site parameter. Other source contributions are not mapped, such as stress drop (e.g., Bindi et al., 2021; Morasca et al., 2023) and near-source velocity pulses (e.g., Sgobba et al., 2021a). Moreover, if the model is defined for a distance metric that does not include the focal depth (e.g., epicentral distance and Joyner-Boore distance), also the focal depth is not mapped in the functional form. Since this latter is not explicitly considered in the reference model, the effects of focal depth in the ground motion will be reflected in the variability of the δB_e residuals. In particular, if the events have a focal depth significantly different from the average of the events in the ITA18 calibration dataset (see Fig. S1 of the electronic supplement), significant biases in the δB_e residuals are expected. Figure 4 presents δB_e curves for selected events of the ITACAext flatfile, each characterized by different focal depths. Figure 4a is relative to the Irpinia earthquake (M 6.9, the strongest event recorded in Italy), located at depth of 15 km, having zero-mean δB_e over all periods. In this case, we do not have any bias on the δB_e residual term because the event is perfectly in agreement with the prediction of the model. In contrast, the residuals for a very shallow (M 4.3; depth 1.65 km, Fig. 4b) and a deep event (M_W 4.6; depth 66 km, Fig. 4c) exhibit peculiar trends with a clear positive bump at long and short periods, respectively. Figure 4d shows that the variability of the δB_e computed from the ITACAext flatfile is significantly greater than τ of the reference ground motion model (ITA18). This is expected considering that we are including events of different tectonic environments in the testing dataset.

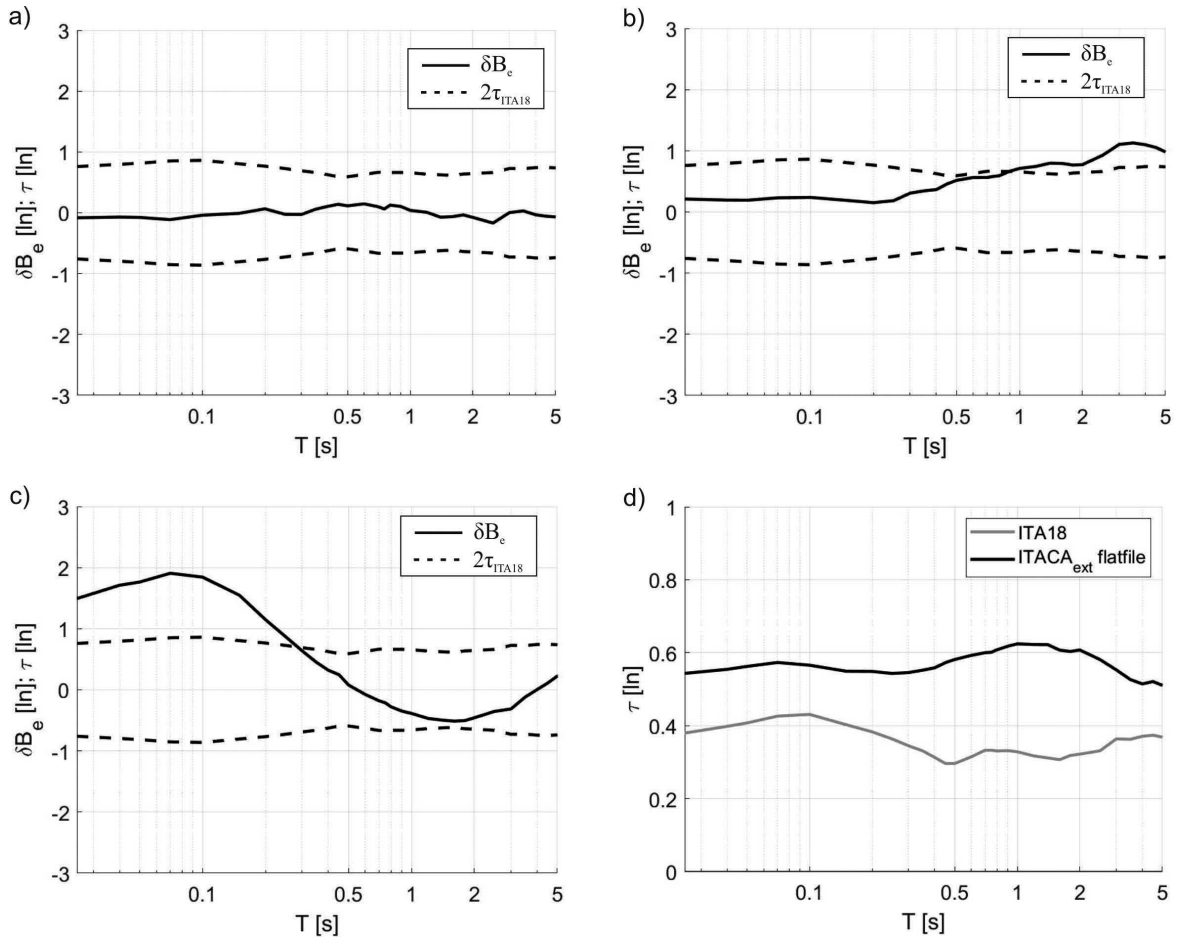

Figure 4. Example of (a) zero-mean δB_e; (b) very shallow event (VSE) relocated by Chiaraluce et al. (2022) at 1.65 km of depth; (c) deep event located in the lithospheric mantle beneath Milan at a depth of 66 Km (Malusà et al., 2022); and (d) ITA18 versus ITACAext between-event standard deviations (τ).

To ensure the reliability of the δB_e estimates, only events with more than 10 associated recordings are considered, resulting in a dataset of 819 δB_e curves from earthquakes with focal depths between 0-470 km and moment magnitudes ranging from 3 to 7. A cluster analysis is applied to the δB_e curves to identify consistent spectral patterns. The resulting clusters are subsequently analyzed as a function of focal depth to evaluate whether, and to what extent, depth influences the spectral characteristics of event-specific ground-motion residuals.

4. Cluster Analysis

The cluster analysis is carried out using two popular unsupervised machine learning algorithms: *k-means* (Lloyd, 1982) and *hierarchical clusters* (Pedrycz, 2011). *K-means* divides data into a predefined number (*k*) of non-overlapping clusters, while *hierarchical clustering* builds a hierarchy of clusters, either by merging smaller clusters or by splitting larger ones. The former can be sensitive to the number of clusters decided beforehand and it works well when the clusters are spherical and equally sized, which may not be ideal for all datasets. The latter does not require choosing the number of clusters beforehand, it should capture more complex structures, but it is also sensitive to outliers. For these reasons, both clustering methods are adopted to explore the systematic trends of the δB_e spectral curves.

In this study, we use the *k-means* algorithm of Hartigan and Wong (1979) implemented in the R software environment (R Core Team, 2017), which requires as input only the array of observations and the number *k* of clusters. The array of observation is composed of 819 objects (δB_e curves), with 31 attributes (i.e., 31 spectral ordinates for an oscillator period T in the range 0.01-5 s). To find the optimal number of clusters, *k*, we apply a statistical

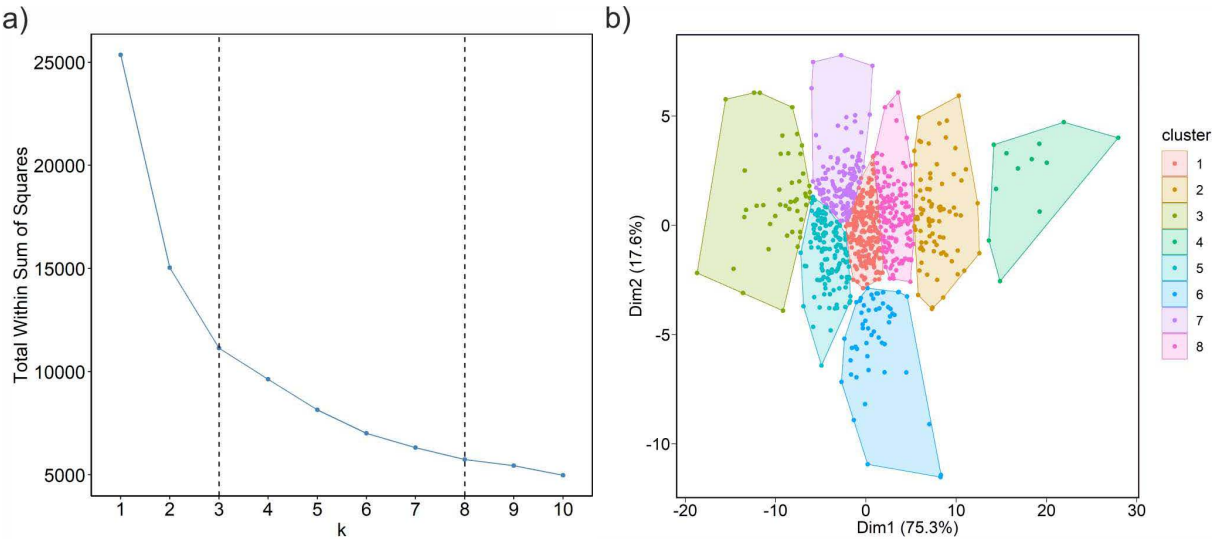

Figure 5. (a) Elbow method optimization algorithm for the determination of k. The vertical dashed lines indicate the range for the optimal determination of k. (b) PCA score plot with $k = 8$. Dim1 and Dim2 indicate the principal component axes.

technique named 'elbow method' (e.g., Sugar, 1998; Sugar et al., 1999), which identifies the most appropriate value of k based on an optimization criterion aimed at the minimization of the within-cluster variability (i.e., total within sum of squares). Figure 5a shows that this method leads to k values between 3 and 8, identified by the bending of the curve. Therefore, to find the optimal k number, we adopt a trail-and-error approach. We start from $k = 3$ and increase the number until the mean curves describing the clusters become similar. We find that $k = 8$ is a good compromise to highlight different behaviors associated with different clusters.

Figure 5b shows the results of the cluster analysis carried out on the δB_e residuals computed on the horizontal components of acceleration response spectra, assuming $k = 8$. The results are displayed through the PCA (Principal Component Analysis) score plots, where each object is depicted as a point in a 2D space and the axes are the first two principal components (hereinafter indicated as Dim1 and Dim2) determined via PCA (e.g., Wells, 2011). The PCA score plot in Fig. 5b clearly indicates distinct separated clusters along Dim1 that explains 75.3 % of the variability in the data, while Dim2 describes 17.6 % only.

Finally, the *hierarchical clustering* algorithm, implemented in the R software environment (R Core Team, 2017), is applied to the same dataset. *Hierarchical clustering* organizes data points into a tree-like structure known as a dendrogram, based on their similarity and distances. The clustering process involves iteratively merging or splitting clusters according to the computed distances, gradually building a hierarchy that is ultimately represented by the dendrogram. To generate this structure, the first step is to compute the distance matrix of the dataset. In this study, dissimilarity is measured using the Euclidean distance. Hierarchical clustering is then performed on this matrix using the average linkage method, which applies an agglomerative (bottom-up) approach: starting with each data point as an individual cluster, the algorithm successively merges the closest clusters until a single cluster encompassing all data points is formed. Once the dendrogram is computed, it can be cut at a chosen level to obtain a specified number of clusters (k). With $k = 8$, as assumed in the *k-means* algorithm, most of the δB_e curves are grouped into a single cluster, with only a few curves forming separate clusters. Given the high sensitivity of this clustering method to outliers, a value of $k = 16$ is ultimately chosen for truncating the dendrogram (see Fig. S2 of the electronic supplement). This allows for a more comprehensive representation, capturing both the main trends and the presence of individual outliers among the δB_e curves.

5. Results

As the cluster analysis of the δB_e spectral curves for the vertical ground-motion components produced results comparable to those of the horizontal components (see Fig. S3 of the electronic supplement), only the latter are

presented below. Figure 6 shows the average δB_e curves for the eight clusters obtained with the *k-means* algorithm. Some clusters have median δB_e that are, on average, within the model variability (τ), whereas other clusters exceed 2τ in a range of periods, or in the entire investigated period range (0.01-5 s). A summary of the main features of each cluster is reported in Table 1.

The yellow curves in Fig. 6, corresponding to the three clusters $Kh = 1,5,8$, are included in the variability of the ITA18 ground motion model ($\pm 2\tau_{ITA18}$) and the δB_e curves do not present any particular trend: one cluster is zero-mean, one is slightly positive, and one is slightly negative. Overall, most of the events of the ITACAext dataset fall in this category, with 494 events out of 819 (213 in $Kh = 1$; 133 in $Kh = 5$; 148 in $Kh = 8$). Events belonging to these clusters do not exhibit any specific spatial clustering across Italy (Fig. 7) or distinct magnitude-depth distributions (Fig. 8), as these are mainly crustal events down to 30 km depth, consistent with those related to the ITA18 calibration dataset (see Fig. S1 of the electronic supplement).

Table 1. Event classification in ITACAext (version 1.0; Brunelli et al., 2022). The clusters are those reported in Fig. 6.

Cluster	Description	Number of events	Main features
$Kh = 2,3$	Anomalous clusters	125	– Average δB_e values around ($\pm 2\tau_{ITA18}$) – Many events have limited seismic station coverage
$Kh = 1,5,8$	ITA18-consistent	494	– δB_e included in the variability of the ITA18 model – δB_e with no particular trend
$Kh = 6$	Very Shallow Events (VSE)	52	– Long-period δB_e is larger than expected – Short-period δB_e is smaller than expected – Focal depth <10 km – Very shallow volcanic events have the lowest negative δB_e values in the short-period range – Possible mislocated events
$Kh = 7$	Deep Crustal Events (DCE)	136	– Short-period δB_e is larger than expected, tending to zero towards the long-periods – Focal depth >10 km
$Kh = 4$	Subduction Events	12	– In-slab events of the Calabrian Arc – Focal depth >100 km

Unlike the clusters previously described, clusters $Kh = 2$ and $Kh = 3$ (green curves in Fig. 6) present anomalous δB_e curves. Indeed, $Kh = 2$ (80 events out of 819) has average δB_e values around -2τ (Fig. 9a), and $Kh = 3$ (45 events out of 819) has average values around $+2\tau$ (Fig. 9b). As observed by Mascandola et al. (2022), many of these events are located abroad, along the Italian border, or along the coast (Fig. 7a), where the poor azimuthal coverage of the stations around the epicenter can be one of the causes of the anomalous δB_e. In these cases, the estimates of the δB_e residuals can be affected by a trade-off with propagation effects.

Among the clusters identified in Fig. 6, the most noteworthy are those exhibiting a peculiar trend. Specifically, clusters $Kh = 6$ and $Kh = 7$ are peculiar because they are characterized by δB_e curves with different behavior for the long- and short-periods. In $Kh = 6$ (Fig. 10a), long-period ground motion is larger than expected (i.e, observations larger than predictions), whereas short-period ground motion is smaller than expected (i.e., observations lower than predictions). This cluster includes 52 out of 819 events and, compared to the other identified clusters, it seems associated with very shallow events (VSE), with focal depth <10 km (Fig. 10b). Most of these are crustal events localized in Central Italy (Fig. 7b), with magnitudes lower than 3.5 and focal depths between 5 and 10 km (Fig. 10b). However, $Kh = 6$ also includes a minority of volcanic events localized in Ischia Island or Mt. Etna (Fig. 7b), with higher magnitudes between 3.5 and 4.5, and even shallower hypocentral depths (<5 km). Volcanic events can be distinguished thanks to the lower negative values (i.e., largest in absolute value) in the short-period range (Fig. 10a). The spatial distribution of this cluster is consistent with the spatial

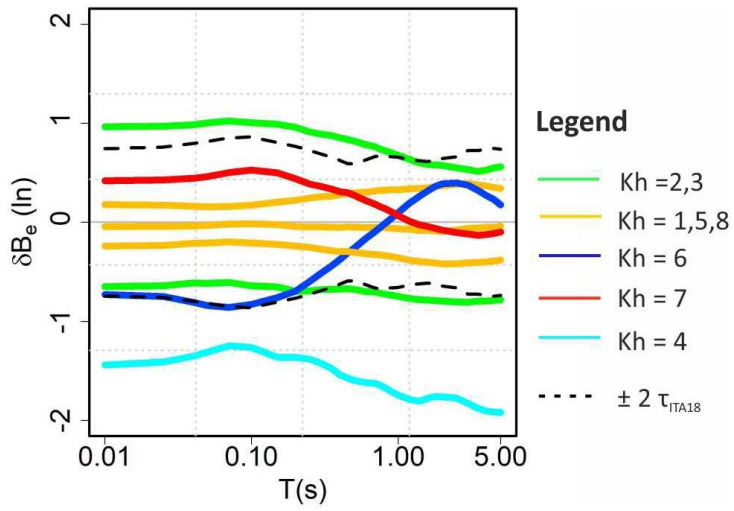

Figure 6. Average curves of the 8 clusters (*Kh*) recognized on the δB_e residuals computed from response spectra of the horizontal ground-motion components. The $\pm 2\tau$ variability of the ITA18 model is also indicated with black dashed lines.

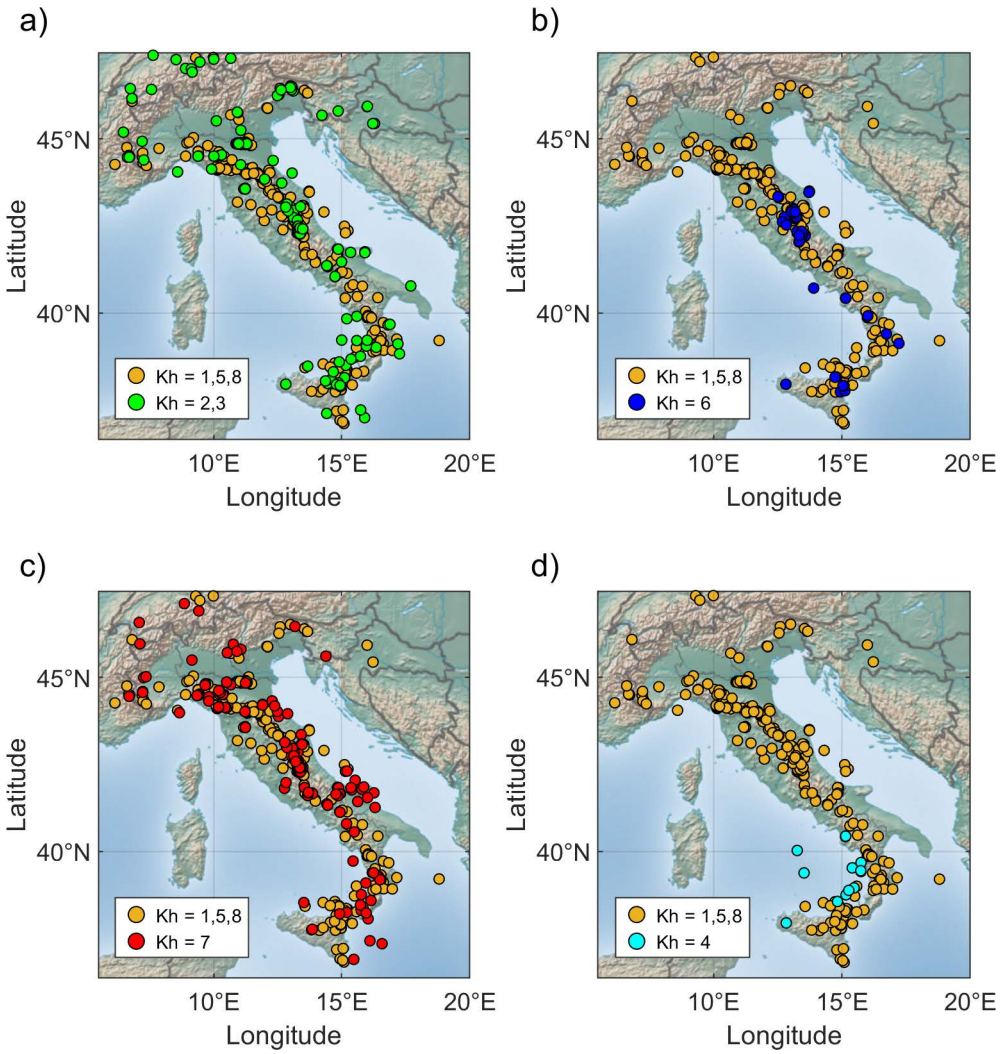

Figure 7. Spatial distribution of the clusters in Fig. 6. The crustal events up to 30 km depth of *Kh* = 1,5,8 are reported in all panels (yellow circles). (a) Anomalous events of *Kh* = 2,3; (b) VSE of *Kh* = 6; (c) Deeper crustal events up to 80 km depth (*Kh* = 7); (d) Subduction events more than 100 km depth (*Kh* = 4).

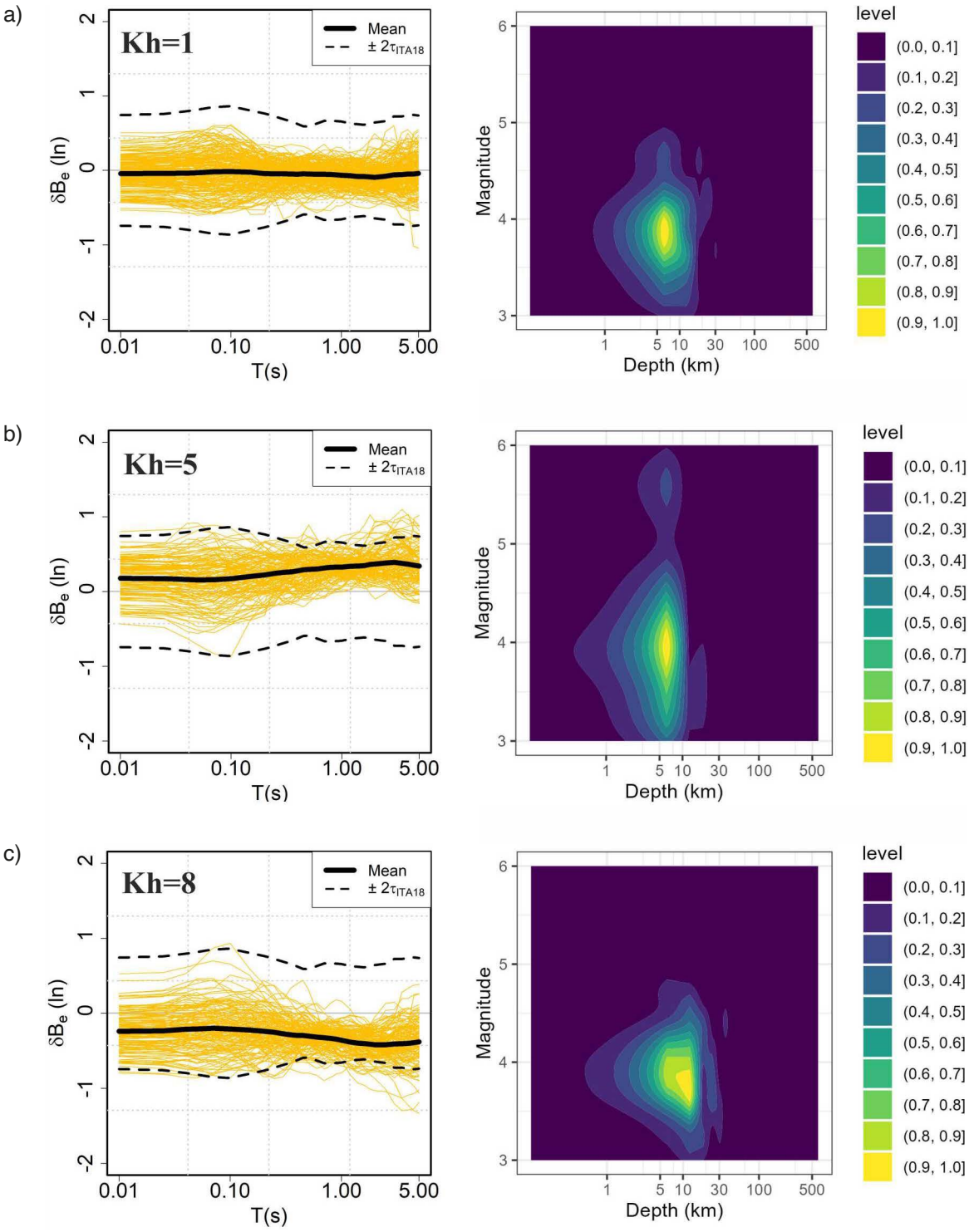

Figure 8. Crustal events down to 30 km depth. $Kh = 1$ (a), $Kh = 5$ (b), and $Kh = 8$ (c) with the corresponding magnitude-depth density plot aside. Left panels: the average curve is reported in black and the $\pm 2\tau$ variability of the ITA18 model is indicated with dashed black lines.

distribution of shallow seismicity in Central Italy (e.g., Michele et al., 2020; Barchi et al., 2021; Chiaraluce et al., 2022) and on the Etna Volcano (e.g., Carlino et al., 2022). While the shallow seismicity of this latter is strictly related to the structure of the volcanic edifice and the magmatic activity, the shallow seismicity in Central Italy has been related to the influence of surface geology (Barchi et al., 2021).

The other cluster with a peculiar shape is $Kh = 7$, which presents an opposite behavior with respect to $Kh = 6$ (Fig. 10c). Indeed, it is characterized by positive δB_e residuals in the short-period range, tending to zero

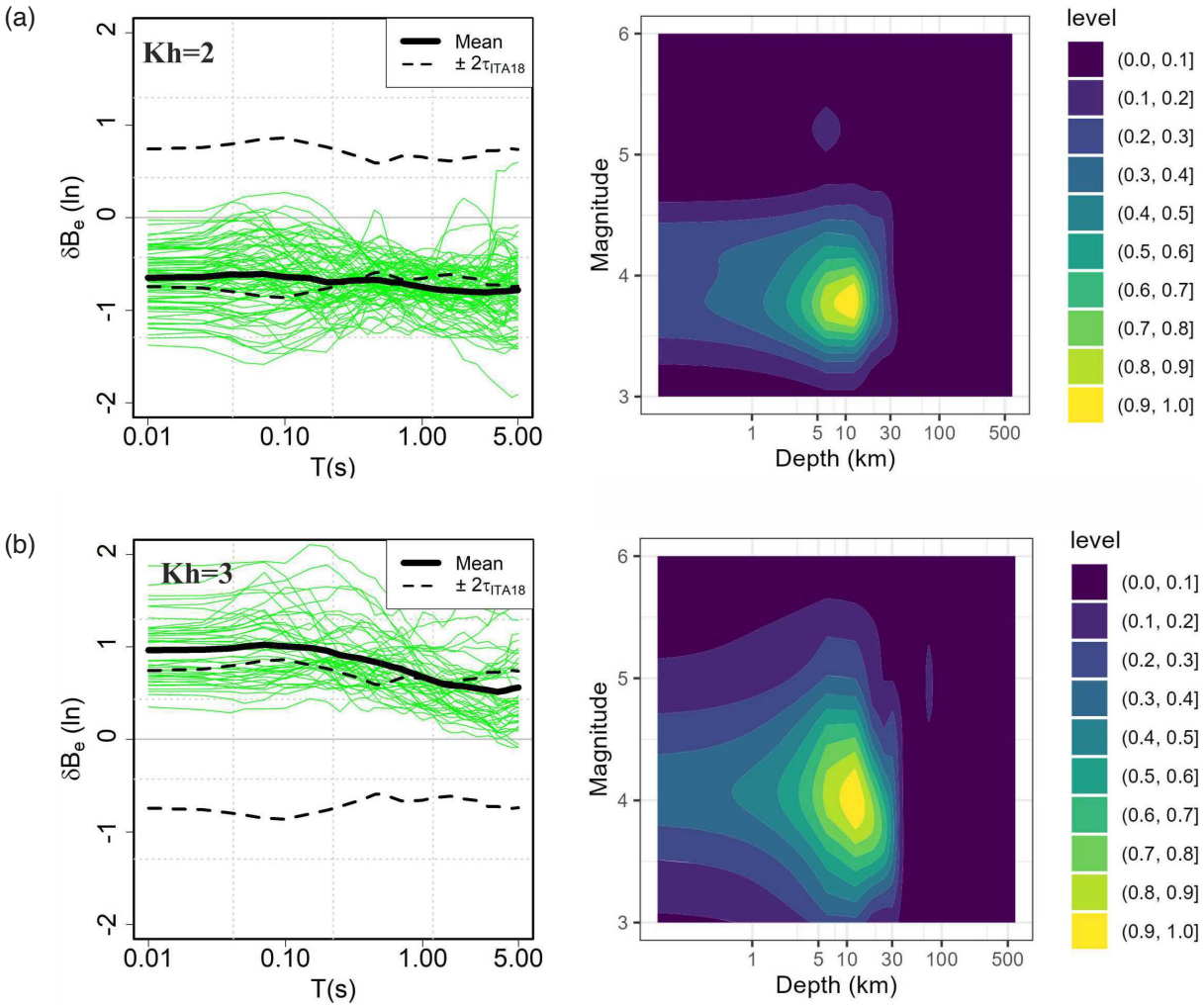

Figure 9. Anomalous clusters. *Kh* = 2 (a) and *Kh* = 3 (b) with the corresponding magnitude-depth density plot aside.

toward long periods. This cluster seems associated with deep crustal events (DCE), with depths generally larger than 10 km (Fig. 10d). In particular, the deeper events (between 25 and 80 km in depth) are characterized by higher positive values in the short-period range (Fig. 10c). Overall, this cluster includes 136 out of 819 events that are mainly localized in the outer sector of the Apennines, in the Gargano Promontory, and in the Calabrian Arc (Fig. 7c), in agreement with other regional studies that relate the deeper seismicity of the Apennines to the subduction of the Adriatic lithosphere (e.g., Chiarabba et al., 2014; D'Acquisto et al., 2020), the deeper seismicity of the Gargano promontory to the presence of fluids (Miccolis et al., 2021; Lavecchia et al., 2022), and the deeper seismicity of the Calabrian Arc to the subduction of the Ionian oceanic crust (e.g., Maesano et al., 2017). In this regard, cluster *Kh* = 4 includes only the in-slab events of the Calabrian Arc, located in the southern Tyrrhenian Sea (Fig. 7d). This cluster includes 12 out of 819 events, with δB_e curves that are well below the -2τ variability of the ITA18 model (Fig. 10e) and hypocenters more than 100 km in depth (Fig. 10f).

The clusters identified by the *k-means* algorithm have been confirmed by *hierarchical clustering*. Therefore, they are not shown here for the sake of brevity. The main difference lies in the greater level of detail provided by *hierarchical clustering*, particularly for deep seismic events. As illustrated on Fig. 11, deep events share a similar δB_e curve shape, corresponding to the DCE cluster ($k = 7$ in Fig. 10c), but exhibit a progressive shift toward more negative values as focal depth increases. Figure 11a-b shows the deep crustal events (DCE) up to 30 km depth. Among these we find the events of the Gargano Promontory. Figure 11c-d shows the mantle events from 30 km to 100 km depth, which include the deep events located in the lithospheric mantle beneath Milan (Malusà et al., 2022), and the deep events in the Ionian Sea, in Southern Italy. The cluster in Fig. 11e-f groups events of different depths (from 10 to 250 km depth), mainly located in correspondence to the Calabrian Arc, and possibly related to the Tyrrhenian subduction. The deepest in-slab events (100-500 km depth) are grouped in a separate cluster reported in Fig. 11 g-h.

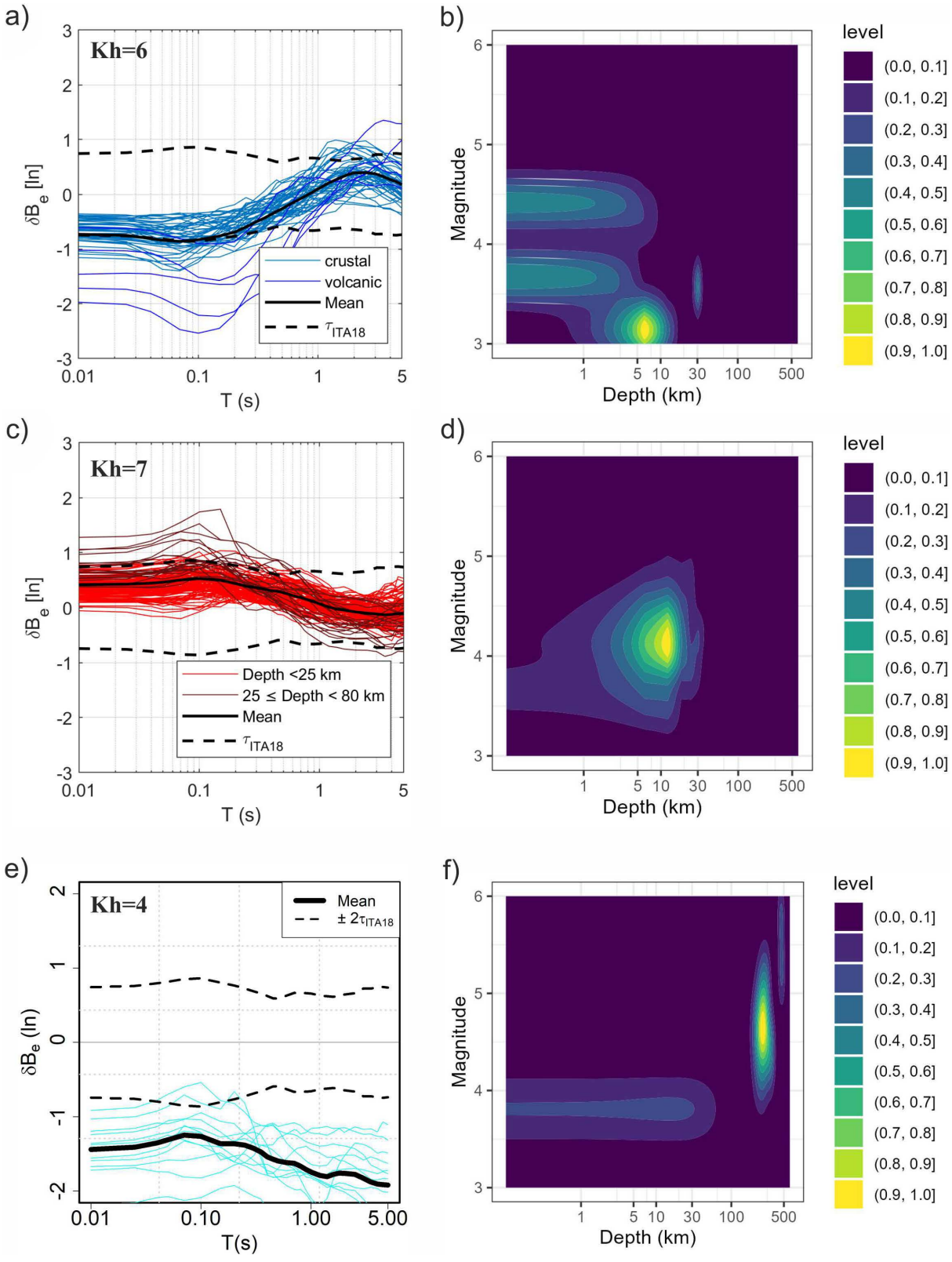

Figure 10. Peculiar clusters on the left (*Kh* = 6,7,4), with the corresponding magnitude-depth density plot on the right.

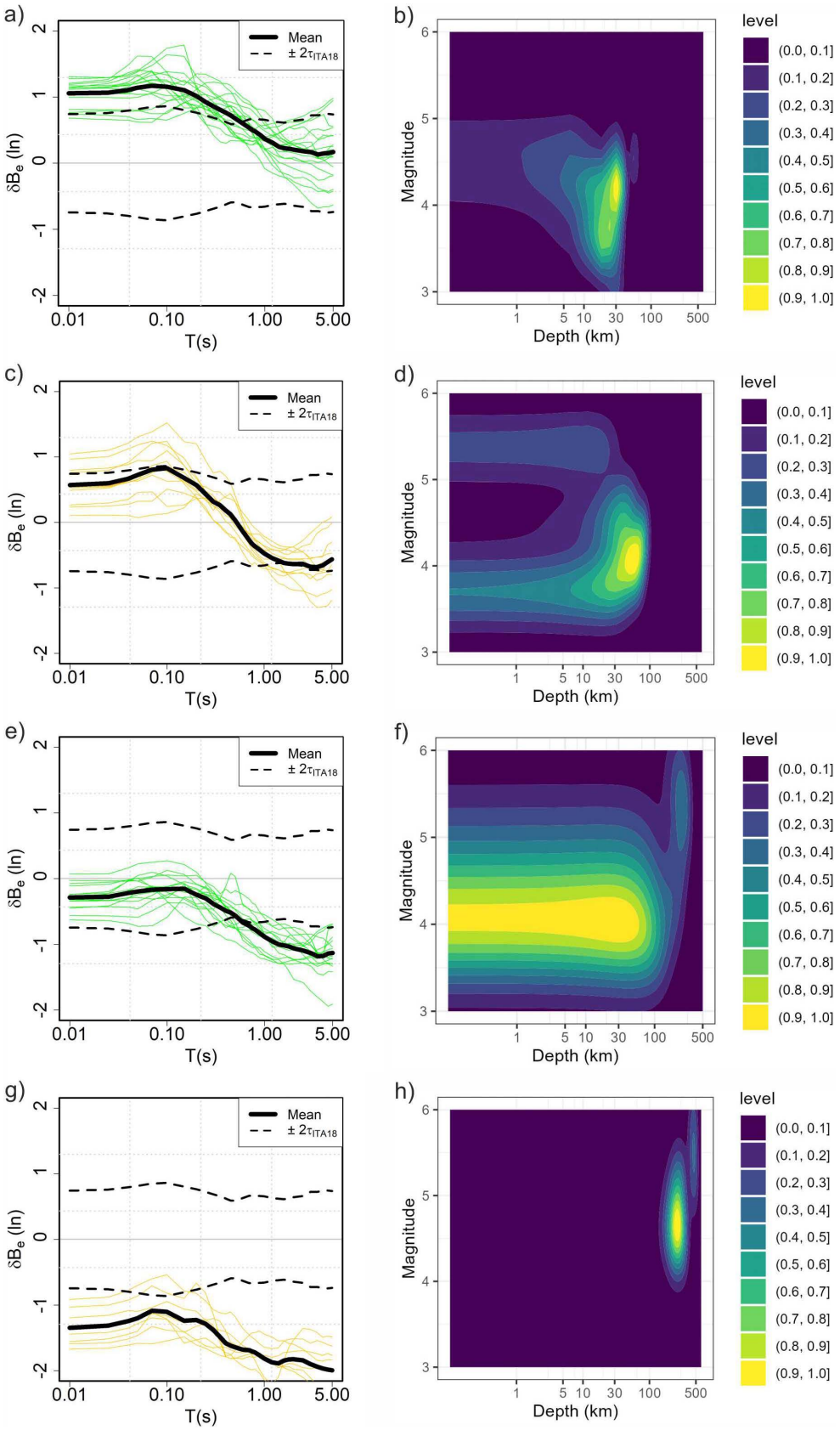

Figure 11. On the left the deep-events clusters recognized by *hierarchical clustering*; on the right the density plots for the magnitude and focal depth distribution of the corresponding events. (a-b) Deep crustal events (DCE) up to 30 km depth; (c-d) mantle events from 30 km to 100 km depth; (e-f) deep events, up to 100 km depth, related to the Tyrrhenian subduction in front of the Calabrian Arc; (g-h) deepest in-slab events (100-500 km depth) of the Tyrrhenian subduction.

6. Discussion

Although depth plays a crucial role in determining the type and characteristics of seismic waves generated during an earthquake, generally this is not well constrained, especially for very shallow events (depth <10 km), and the uncertainty on focal depth is reflected in the variability of the event-specific ground-motion residuals, δB_e. Indeed, the cluster analysis performed on the δB_e residuals of the ITACAext flatfile identified different trends that can be related to the depth of the earthquakes (see Table 1). In particular, the peculiar shapes found in this study for the δB_e residuals of VSE and DCE may be adopted as a proxy for identifying mislocated events or detecting earthquakes that have been erroneously classified as shallow crustal seismicity.

In shallow earthquakes, ground motions tend to exhibit higher low-frequency energy content compared to those generated by deeper events. This results in a systematic effect observable in the δB_e curves, which show a spectral bump centered at periods greater than 1 second (cluster of VSE – k = 6 in Fig. 10). A possible explanation lies in the large amount of surface waves generated when the hypocenter is located at shallow depth. In such cases, a significant portion of the seismic energy – comprising direct, reflected, and converted waves – reaches the free surface more efficiently and is effectively transformed into Rayleigh and Love waves, which can then propagate over long distances along the Earth's surface (e.g., Lay and Wallace, 1995; Ammon and Anderson, 1991).

To support this interpretation, Fig. 12 shows the velocity waveforms for two earthquakes located at different depths in the Etna area, while Fig. 13 compares the spectrograms observed at the same station (EVRN) during these two events. The first event, a magnitude 4.4 earthquake with a focal depth of 0.3 km, clearly displays pronounced surface-wave energy, as evidenced by the extended signal duration and enhanced low-frequency amplitudes in the waveform. In contrast, the second event, with similar magnitude (M_W 4.5) but a focal depth of 20 km, exhibits a waveform dominated by shorter, high-frequency body waves. The spectrograms reinforce this observation, showing a concentration of energy below 1 Hz for the shallow event, consistent with the generation of surface waves. This enrichment in long-period content (1-10 s) is a distinctive feature of volcanic seismicity, as previously noted by Milana et al. (2008), who linked it to the shallow source depth. Importantly, given the relatively homogeneous volcanic substrate in the epicentral area – dominated by alternating lava flows – local site effects are unlikely to be responsible for the observed differences. Therefore, the contrasting spectral and temporal characteristics of the two events can be reasonably attributed to differences in focal depth and associated wave propagations.

Another peculiar feature of VSE events, in particular of volcanic events, is the depletion of the radiated high-frequencies (i.e. short periods) energy. A plausible explanation for this depth dependence in the event-term residuals, also observed in Bindi et al. (2023a), involves both attenuation effects and source-related properties. On one hand, attenuation is known to decrease with depth, with a more pronounced effect at intermediate to high frequencies (e.g., Bindi et al., 2023a). However, most ground-motion models (e.g., Atkinson et al., 2016) and spectral decomposition approaches, such as the generalized inversion technique (GIT; Oth et al., 2011), do not explicitly incorporate this depth dependence. Therefore, variations in attenuation with depth may be partially absorbed by the event-term residuals (δB_e) in ground-motion modeling, or may bias the estimation of source parameters, such as stress drop in GIT-based analyses (e.g., Abercrombie et al., 2021; Bindi et al., 2023b).

On the other hand, source properties themselves may vary with depth. Ji et al. (2024) demonstrated a significant increase in both apparent stress and dynamic stress drop with increasing centroid depth, independent of attenuation effects. Specifically, they found that deeper earthquakes (depth >6 km) exhibit apparent and dynamic stress drops nearly four times higher than those of shallower events. Given the strong correlation between short-period δB_e and stress drop, the depth dependence of source parameters may also emerge through residual analysis.

The relation between short-period δB_e residuals and source parameters is tested in Fig. 14, where about 100 relocated events (M 3.1-6.5) in Central Italy, derived from CAT3 catalog of Chiaraluce et al. (2022), are selected. Figure 14a-b shows the between-event residuals plotted as a function of focal depth and colored according to the source parameters ($\Delta\sigma$ and κ_{source}) estimated by Morasca et al. (2023) using a generalized inversion technique not considering the attenuation decrease with depth. Although the selected events are all located within 12 km depth, a depth dependence of high-frequency between-event residuals, stress drop, $\Delta\sigma$, and high-frequency attenuation at the source, κ_{source}, is observed. As reported in previous studies (Bindi and Kotha, 2020; Morasca et al., 2023; Brunelli et al., 2023), the residuals increase as the values of $\Delta\sigma$ increase and decrease as the values of κ_{source} increases (Fig. 14c-d), event if according to the outcomes of Abercrombie et al. (2021) and Bindi et al. (2023), these relations can be an artifact of neglecting depth-dependence of attenuation properties.

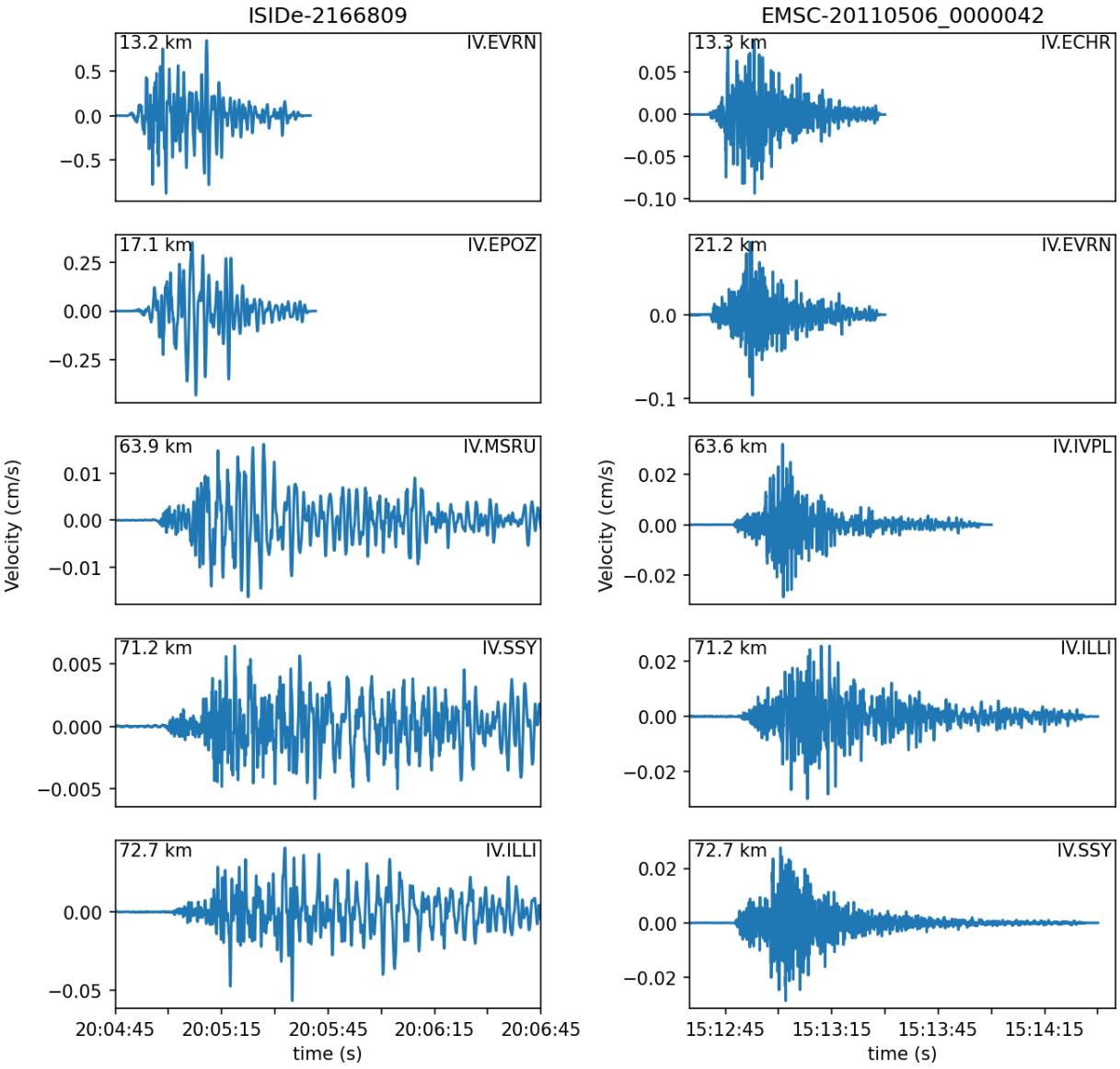

Figure 12. Velocimetric time histories of the ISIDe-2166809-0.3 km in depth (left) and EMSC-20110506_0000042-20 km in depth (right) events. Records are sorted for epicentral distance and relate to 2 minutes of signal starting from the origin time.

Finally, to validate the spectral shapes of δB_e previously identified, a cluster analysis is applied also on the dataset of relocated events in Central Italy, confirming the δB_e spectral shapes previously obtained (Fig. S4 of the electronic supplement). In particular, two clusters are similar to the VSE and DCE clusters identified on the ITACAext flatfile. The colored circles in Fig. 14c-d indicate the earthquakes belonging to the VSE (blue) and DCE (red) clusters identified in Central Italy. The former with focal depths ranging between 0 and 3 km, the latter with focal depths ranging between 3 and 12 km. Unlike the ITACAext, where the depth threshold between these two clusters was around 10 km (based on non-relocated depths), in this case the depth threshold is around 3 km.

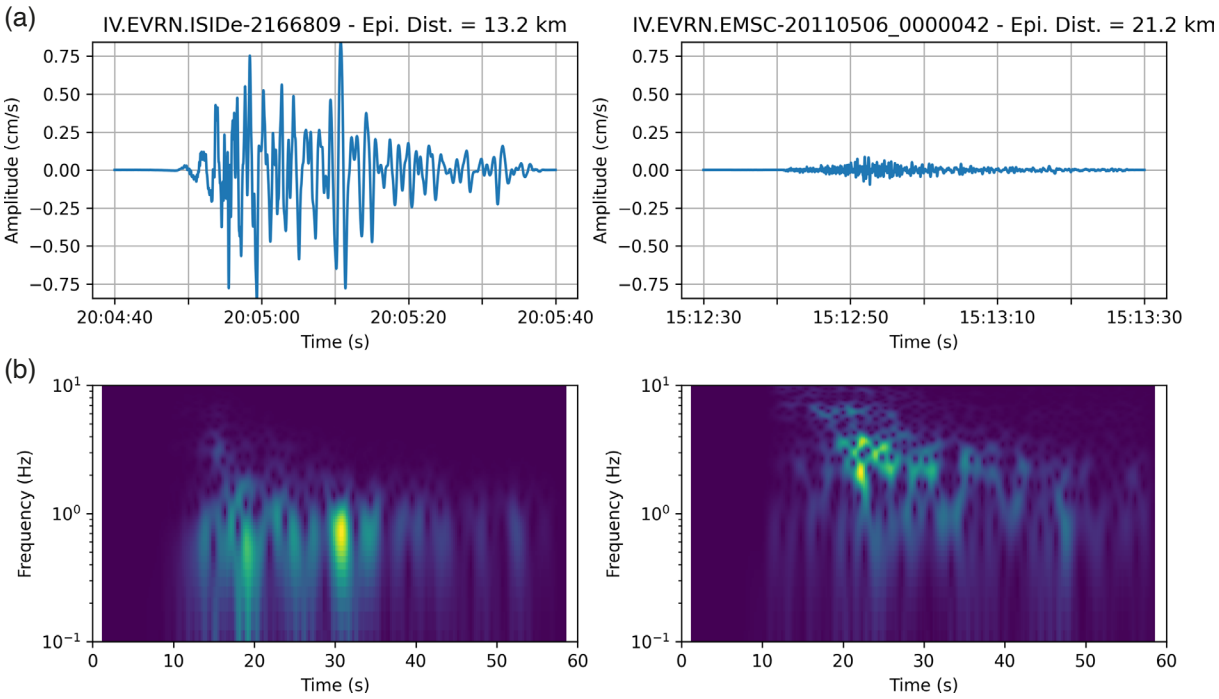

Figure 13. Velocimetric time histories of the IV.EVRN records of ISIDe-2166809 and EMSC-20110506_0000042 events (a), with the corresponding spectrograms in (b).

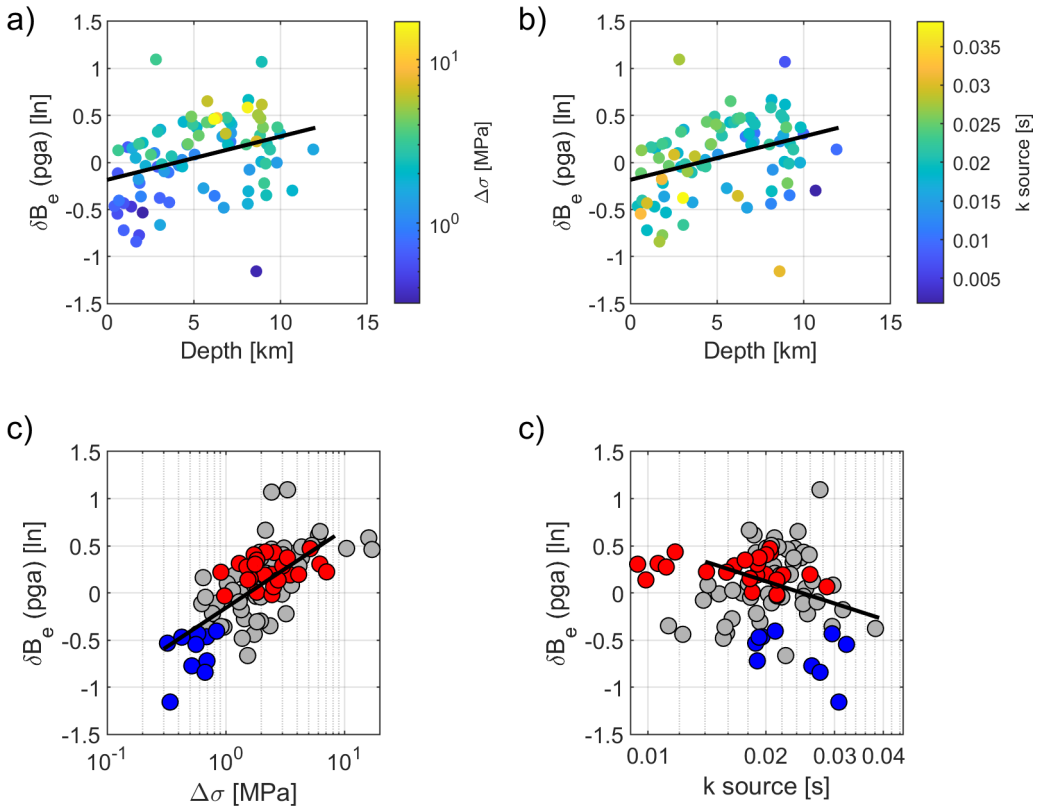

Figure 14. δB_e residuals at Peak Ground Acceleration (pga) versus depth, colored according to stress drop, $\Delta\sigma$ (a) and high-frequency attenuation at the source κ_{source} (b), as estimated by Morasca et al. (2023) for a set of events in Central Italy. The depth are those provided by Chiaraluce et al. (2022) in CAT3 catalog. δB_e residuals at Peak Ground Acceleration (pga) versus stress drop, $\Delta\sigma$ (c), and high-frequency attenuation at the source κ_{sourc} (d), with the VSE cluster highlighted in blue and the DCE cluster highlighted in red.

7. Conclusions

Given the high uncertainty on focal depths estimations, in this study we analyzed the event-specific ground-motion residuals (i.e., between-event term, δB_e), computed with respect to the latest ground-motion models for shallow crustal earthquakes in Italy (ITA18 in Joyner-Boore distance, Lanzano et al., 2019), to explore whether they can be adopted as a proxy for focal depth.

Ground-motion residuals were computed using the ITACAext flatfile (Brunelli et al., 2022), including events from various tectonic settings, such as volcanic, subduction, and shallow crustal seismicity, despite the reference ground-motion model is calibrated only for shallow crustal events. This approach enables the distinction among different tectonic regimes, which are characterized by distinct depth distributions (e.g., volcanic events are typically very shallow, while subduction events are associated with much deeper seismicity). To ensure robustness, only δB_e with more than 10 records were considered and the magnitude estimates were homogenized into moment magnitude (M_W) from the RCMT (Regional Centroid Moment Tensor; Pondrelli et al., 2002) method. Overall, we analyzed 819 δB_e curves for events ranging between 0-470 km depth and magnitude between 3 and 7. To investigate the relation between the spectral shape of the δB_e residuals and focal depth, a cluster analysis was performed, considering two different methods, i.e. *k-means* and *hierarchical clustering*, obtaining very similar results.

Among the 819 δB_e curves analyzed in this study, 494 are consistent with the ITA18 model – that is, their δB_e values fall within the model variability and do not exhibit any specific trend. A total of 125 curves is classified as anomalous, with δB_e values around $\pm 2\tau_{ITA18}$, likely due to uneven station coverage around the epicenter or metadata inaccuracies. Fifty-two curves are associated with very shallow earthquakes (VSE), possibly mislocated, with focal depths less than 10 km; 136 correspond to deep crustal events (DCE) with focal depths greater than 10 km; and 12 are subduction events from the Calabrian Arc, characterized by focal depths exceeding 100 km and by extremely negative δB_e residuals across the entire spectral period range. VSEs are distinguished by δB_e amplitudes that are systematically positive at long periods (>1 s) and negative at short periods (<1 s), whereas deeper events exhibit the opposite behavior, with δB_e amplitudes decreasing progressively with depth. Volcanic events, in particular, are clearly identifiable within the VSE cluster, showing marked attenuation in short-period ground motion.

Based on these results, the approach proposed in this study appears to be a promising tool for identifying mislocated events or detecting earthquakes erroneously classified as shallow crustal seismicity. The method, which is particularly effective when focal depth uncertainty is significant, can be adopted to improve catalog metadata. This would be beneficial for the definition of a robust calibration dataset for the development of ground motion models. Indeed, Atkinson et al. (2016) showed that a difference of a few km in depth can result in a significant difference in the amplitude of near-source ground-motion. Moreover, the identification of very shallow events has important implications also on hazard estimates. This is related to both the impact of ground-motion models and the different scaling relations of shallow events, as Di et al. (2023) highlighted that very shallow events (≤3 km) are characterized by surface ruptures with abnormally large length and slip. In these cases, the classical scaling relation of Wells and Coppersmith (1994) may not be applicable, and the correct recognition of very shallow events may become an important task to refine the hazard estimates.

Since residual analysis can be automatically performed shortly after an event occurs, and δB_e curves may serve as a proxy for the rapid identification of mislocated events or inaccurate event metadata, as a future application a web service is currently under development to provide this information in near quasi real-time.

Data availability statement. The ITACAext flatfile is available on the ITalian ACcelerometric Archive (ITACA; https://itaca.mi.ingv.it/) at the following link: https://itaca.mi.ingv.it/ItacaNet_40/#/products/itacaext_flatfile. The hypocentral coordinates of the Italian events are provided by the INGV surveillance service at http://terremoti.ingv.it/. Hypocentral positions from the European-Mediterranean Seismological Centre (EMSC-CSEM) are available at https://www.seismicportal.eu/, whereas those from the International Seismological Centre (ISC) are available at www.isc.ac.ukISC.

Acknowledgements. This research was partially supported by Istituto Nazionale di Geofisica e Vulcanologia (INGV) in the frame of the project SECURE – within Pianeta Dinamico (Working Earth) – Geosciences for the Understanding of the Dynamics of the Earth and the Consequent Natural Risks, founded by the Italian Ministry of University and Research (MIUR) and in the frame of the agreement with EDF (Electricité de France), aimed at characterizing the seismic ground motion in near source conditions for moderate-to-large magnitudes.

References

Abercrombie, R. E., D. T. Trugman, P. M Shearer, X. Chen et al. (2021). Does earthquake stress drop increase with depth in the crust?, J. Geophys. Res. Solid Earth, 126, e2021JB022314, doi:10.1029/2021JB022314.

Al-Atik, L., N. A. Abrahamson, J. J. Bommer, F. Scherbaum et al. (2010). The variability of ground-motion prediction models and its components, Seismol. Res. Lett., 81, 5, 794-801, doi:10.1785/gssrl.81.5.794.

Atkinson, G. M., E. Yenier, N. Sharma and V. Convertito (2016). Constraints on the near-distance saturation of ground-motion amplitudes for small-to-moderate induced earthquakes, Bull. Seismol. Soc. Am., 106, 5, 2104-2111, doi:10.1785/0120160075.

Barchi, M. R., F. Carboni, M. Michele, M. Ercoli et al. (2021). The influence of subsurface geology on the distribution of earthquakes during the 2016-2017 Central Italy seismic sequence, Tectonophysics, 807, 228797, doi:10.1016/j.tecto.2021.228797.

Bates, D., M. Mächler, B. Bolker and S. Walker (2014). Fitting linear mixed-effects models using lme4, 67, 1, 1-48, doi:10.18637/jss.v067.i01.

Bindi, D., L. Luzi, P. Pacor and R. Paolucci (2011). Identification of accelerometric stations in ITACA with distinctive features in their seismic response, Bull. Earthq. Eng., 9, 1921-1939, doi:10.1007/s10518-011-9271-5.

Bindi, D., S. R. Kotha, G. Weatherill, G. Lanzano et al. (2019). The pan-European engineering strong motion (ESM) flatfile: consistency check via residual analysis, Bull. Earthq. Eng., 17, 583-602, doi:0.1007/s10518-018-0466-x.

Bindi, D., H. N. Razafindrakoto, M. Picozzi and A. Oth (2021). Stress drop derived from spectral analysis considering the hypocentral depth in the attenuation model: Application to the Ridgecrest region, California. Bull. Seismol. Soc. Am., 111, 6, 3175-3188, doi:10.1785/0120210039.

Bindi, D., D. Spallarossa, M. Picozzi, A. Oth et al. (2023a). The Community Stress-Drop Validation Study – Part I: Source, Propagation, and Site Decomposition of Fourier Spectra, Seismol. Res. Lett., 94, 4, 1980-1991, doi:10.1785/0220230019.

Bindi, D., D. Spallarossa, M. Picozzi, A. Oth et al. (2023b). The Community Stress-Drop Validation Study – Part II: Uncertainties of the Source Parameters and Stress Drop Analysis, Seismol. Res. Lett., 94, 4, 1992-2002, doi:10.1785/0220230020.

Brunelli, G., G. Lanzano, M. C. D'Amico, C. Felicetta et al. (2022). ITACAext Flat-file: tabelle di metadati e parametri relativi allo scuotimento sismico (Data Set), Istituto Nazionale di Geofisica e Vulcanologia, Milano, Italy, doi:10.13127/itaca32/itacaext_flatfile.1.0.

Brunelli, G., G. Lanzano, L. Luzi and S. Sgobba (2023). Data-driven zonations for modelling the regional source and propagation effects into a Ground Motion Models in Italy, Soil Dyn. Earthq. Eng., 166, 107775, doi:10.1016/j.soildyn.2023.107775.

Caciagli, M., R. Camassi, S. Danesi, S. Pondrelli et al. (2015). Can we consider the 1951 Caviaga (northern Italy) earthquakes as noninduced events?, Seismol. Res. Lett., 86, 5, 1335-1344, doi:10.1785/0220150001.

Carlino, F., M., L. Scarfì, F. Cannavò, G. Barberi et al. (2022). Frequency-magnitude distribution of earthquakes at Etna volcano unravels critical stress changes along magma pathways, Commun. Earth Environ., 3, 1, 68, doi:10.1038/s43247-022-00398-6.

Castro, R. R., F. Pacor and D. Spallarossa (2021). Depth-Dependent Shear-Wave Attenuation in Central Apennines, Italy, Pure Appl. Geophys., 178, 2059-2075, doi:10.1007/s00024-021-02744-9.

Chiarabba, C., G. Giacomuzzi, I. Bianchi, N. P. Agostinetti et al. (2014). From underplating to delamination-retreat in the northern Apennines, Earth Planet. Sci. Lett., 403, 108-116, doi:10.1016/j.epsl.2014.06.041.

Chiaraluce, L., M. Michele, F. Waldhauser, Y. J. Tan et al. (2022). A comprehensive suite of earthquake catalogues for the 2016-2017 Central Italy seismic sequence, Sci. Data, 9, 1, 710, doi:10.1038/s41597-022-01827-z.

D'Acquisto, M., L. Dal Zilio, I. Molinari, E. Kissling et al. (2020). Tectonics and seismicity in the Northern Apennines driven by slab retreat and lithospheric delamination, Tectonophysics, 789, 228481, doi:10.1016/j.tecto.2020.228481.

De Luca, G., M. Cattaneo, G. Monachesi and A. Amato (2009). Seismicity in the Umbria-Marche region from the integration of national and regional seismic networks. Tectonophysics, 476, 1, 219-231, doi:10.1016/j.tecto.2008.11.032.

Di, N., C. Li, T. Li, W. Hu et al. (2023). The 2021 M_W 5.2 Baicheng Earthquake: Implications for the Hazards of Extremely Shallow Earthquakes, Seismol. Res. Lett., 94, 4, 1775-1790, doi:10.1785/0220220328.

Dreger, D. S. (2003). Time-domain moment tensor INVerse codel (TDMT-INVC) release 1.1., W. H. K. Lee, H. Kanamori, P. C. Jennings and C. Kisslinger (Editors), Int. Handb. Earthq. Eng. Seismol., B, 1627, Academic Press, Amsterdam, 1627, 9780124406520.

Eva, E., M. G. Malusà and S. Solarino (2020). Seismotectonics at the transition between opposite-dipping slabs (western Alpine region), Tectonics, 39, 9, e2020TC006086, doi:10.1029/2020TC006086.

Franceschina, G. and A. Tento (2023). High frequency attenuation of S waves in alluvial deposits of the central Po Plain (northern Italy), Geophys. Journal International, 234, 3, 2075-2094, doi:10.1093/gji/ggad185.

Gasperini, P., B. Lolli and G. Vannucci (2013). Empirical calibration of local magnitude data sets versus moment magnitude in Italy, Bull. Seismol. Soc. Am., 103, 4, 2227-2246, doi:10.1785/0120120356.

Gomberg, J. S., K. M. Shedlock and S. W. Roecker (1990). The effect of S-wave arrival times on the accuracy of hypocenter estimation, Bull. Seismol. Soc. Am., 80, 6A, 1605-1628, doi:10.1785/BSSA08006A1605.

Hartigan, J. A. and M. A. Wong (1979). Algorithm AS136: a K-means clustering algorithm, J. R. Stat. Soc. C Appl. Stat, 28, 1, 100-108, doi:10.2307/2346830.

ISIDe Working Group (2007). Italian Seismological Instrumental and Parametric Database (ISIDe), Istituto Nazionale di Geofisica e Vulcanologia (INGV), https://data.ingv.it/dataset/09#additional-metadata.

Janský, J., J. Zahradník and V. Plicka (2009). Shallow earthquakes: Shallower than expected?, Stud. Geophys. Geod., 53, 2, 261, doi:10.1007/s11200-009-0016-8.

Ji, C., R. J. Archuleta and A. Peyton (2024). Capturing Broadband Spectral Characteristics of Moderate-Size Earthquakes Using Nearby Recordings: A Case Study of 42 Mw 4.0-5.4 Ridgecrest Earthquakes, Bull. Seismol. Soc. Am., 115, 3, 850-874., doi:10.1785/0120240180.

Joyner, W. B. and D. M. Boore (1981). Peak horizontal acceleration and velocity from strong-motion records including records from the 1979 Imperial Valley, California earthquake, Bull. Seismol. Soc. Am. 71, 6, 2011-2038, doi:10.1785/BSSA0710062011.

Karakostas, V., O. Tan, A. Kostoglou, E. Papadimitriou et al. (2021). Seismotectonic implications of the 2020 Samos, Greece, Mw 7.0 mainshock based on high-resolution aftershock relocation and source slip model, Acta Geophys., 69, 979-996, doi:10.1007/s11600-021-00580-y.

Kotha, S. R., G. Weatherill, D. Bindi and F. Cotton (2020). A regionally-adaptable ground-motion model for shallow crustal earthquakes in Europe, Bull. Earthq. Eng., 18, 9, 4091-4125, doi:10.1007/s10518-020-00869-1.

Lanzano, G., L. Luzi, F. Pacor, C. Felicetta et al. (2019). A Revised Ground-Motion Prediction Model for Shallow Crustal Earthquakes in Italy, Bull. Seismol. Soc. Am., 109, 525-540, doi:10.1785/0120180210.

Lanzano, G., C. Felicetta, F. Pacor, D. Spallarossa et al. (2020). Methodology to identify the reference rock sites in regions of medium-to-high seismicity: an application in Central Italy, Geophys. J. Int., 222, 3, 2053-2067, doi:10.1093/gji/ggaa261.

Lanzano, G., C. Felicetta, F. Pacor, D. Spallarossa et al. (2022). Generic-To-Reference Rock Scaling Factors for Seismic Ground Motion in Italy, Bull. Seismol. Soc. Am, 112, 3, 1583-1606, doi:10.1785/0120210063.

Lanzano, G., L. Vitrano, D. Bindi, C. Felicetta et al. (2025). ITACAext 2.0: A High-Quality Parametric Table of Strongto-Weak Motion Recordings for Seismological and Engineering Research in Italy, Seismol. Res. Lett., 1-22, doi:10.1785/0220240309.

Latorre, D., R. Di Stefano, B. Castello, M. Michele et al. (2023). An updated view of the Italian seismicity from probabilistic location in 3D velocity models: The 1981-2018 Italian catalog of absolute earthquake locations (CLASS), Tectonophysics, 846, 229664, doi:10.1016/j.tecto.2022.229664.

Lavecchia, A., M. Filippucci, A. Tallarico, G. Selvaggi et al. (2022). Role of crustal fluids and thermo-mechanical structure for lower crustal seismicity: The Gargano Promontory (southern Italy), Glob. Planet. Change, 217, 103929, doi:10.1016/j.gloplacha.2022.103929.

Lay, T. and T. C. Wallace (1995). Modern Global Seismology, Academic Press, San Diego, 1-551, 0-12-732870-X.

Liou, I. and N. Abrahamson (2024). Framework for Aleatory Variability and Epistemic Uncertainty for the Ground-Motion Characterization Based on the Level of Simplification, Bull. Seismol. Soc. Am. 115, 1, 296-314, doi:10.1785/0120240141.

Lloyd, S. (1982). Least squares quantization in PCM, IEEE trans. Inf. Theory, 28, 2, 129-137, doi: 10.1109/TIT.1982.1056489.

Maesano, F., M. M. Tiberti and R. Basili (2017). The Calabrian Arc: three-dimensional modelling of the subduction interface, Sci. Rep., 7, 1, 8887, doi:10.1038/s41598-017-09074-8.

Malusà, M. G., E. Brandmayr, G. F. Panza, F. Romanelli et al. (2022). An explosive component in a December 2020 Milan earthquake suggests outgassing of deeply recycled carbon. Communications Earth & Environment, 3, 1, 5, doi:10.1038/s43247-021-00336-y.

Margheriti, L., C. Nostro, O. Cocina, M. Castellano et al. (2021). Seismic Surveillance and Earthquake Monitoring in Italy, Seismol. Res. Lett., 92, 3, 1659-1671, doi:10.1785/0220200380.

Mascandola, C., G. Lanzano and F. Pacor (2022). Consistency Check of ITACAext, the Flatfile of the Italian Accelerometric Archive, Geosciences, 12, 9, 334, doi:10.3390/geosciences12090334.

Menichelli, I., P. De Gori, F. P. Lucente, L. Improta et al. (2022). Minimum 1D VP and VP/VS models and hypocentral determinations in the central Mediterranean area, Seismol. Res. Lett., 93, 5, 2670-2685, doi:10.1785/0220220079.

Miccolis, S., M. Filippucci, S. De Lorenzo, A. Frepoli et al. (2021). Seismogenic Structure Orientation and Stress Field of the Gargano Promontory (Southern Italy) From Microseismicity Analysis, Front. Earth Sci., 9, 179, doi:10.3389/feart.2021.589332.

Michele, M., L. Chiaraluce, R. Di Stefano and F. Waldhauser (2020). Fine-scale structure of the 2016-2017 Central Italy seismic sequence from data recorded at the Italian National Network, J. Geophys. Res. Solid Earth, 125, e2019JB018440, doi:10.1029/2019JB018440.

Michele, M., R. Di Stefano, L. Chiaraluce D. Latorre et al. (2023). CARS-Catalog of Relative Seismic Locations of 1981-2018 Italian Seismicity, EGU23, the 25th EGU General Assembly, Copernicus Meetings, Vienna, Austria, Online, doi:10.5194/egusphere-egu23-14033.

Milana, G., A. Rovelli, A. De Sortis, G. Calderoni, et al. (2008). The role of long-period ground motions on magnitude and damage of volcanic earthquakes on Mt. Etna, Italy, Bull. Seismol. Soc. Am., 98, 6, 2724-2738, doi:10.1785/0120080072.

Morasca, P., M. D'Amico, S. Sgobba, G. Lanzano et al. (2023). Empirical correlations between an FAS non-ergodic ground motion model and a GIT derived model for Central Italy, Geophys. J. Int., 233. 1, 51-68, doi:10.1093/gji/ggac445.

Pacor, F., D. Spallarossa, A. Oth, L. Luzi et al. (2016). Spectral models for ground motion prediction in the L'Aquila region (central Italy): evidence for stress-drop dependence on magnitude and depth, Geophys. J. Int., 204, 2, 716-737, doi:10.1093/gji/ggv448.

Parker, G. A., J. P. Stewart, D. M. Boore, G. M. Atkinson et al. (2022). NGA-subduction global ground motion models with regional adjustment factors. Earthq. Spectra, 38, 1, 456-493, doi:10.1177/87552930211034889.

Pedrycz, W. (2011), Introducing WIREs Data Mining and Knowledge Discovery, WIREs Data Mining Knowl Discov., 1, 1-1, doi:10.1002/widm.17.

Peruzza, L., A. Schibuola, M. A. Romano, M. Garbin et al. (2021). A revised image of the instrumental seismicity in the Lodi area (Po Plain, Italy), Solid Earth, 12, 9, 2021-2039, doi:10.5194/se-12-2021-2021.

Pondrelli, S., A. Morelli, G. Ekström, S. Mazza et al. (2002). European-Mediterranean regional centroid-moment tensors: 1997-2000, Phys. Earth Planet. In., 130, 1-2, 71-101, doi:10.1016/S0031-9201(01)00312-0.

Priolo, E., F. Pacor, D. Spallarossa, G. Milana et al. (2020). Seismological analyses of the seismic microzonation of 138 municipalities damaged by the 2016-2017 seismic sequence in Central Italy, Bull. Earthq. Eng., 18, 5553-5593, doi:10.1007/s10518-019-00652-x.

R Core Team (2017). R: A language and environment for statistical computing, R Foundation for Statistical Computing, Vienna, Austria, https://www.R-proje ct.org/.

Ramadan, F., C. Smerzini, G. Lanzano and F. Pacor (2021). An empirical model for the vertical-to-horizontal spectral ratios for Italy, Earthq. Eng. Struct. Dyn., 50, 15, 4121-4141, doi:10.1002/eqe.3548.

Russo, E., C. Felicetta, M. D'Amico, S. Sgobba et al. (2022). Italian Accelerometric Archive v3.2; Istituto Nazionale di Geofisica e Vulcanologia, Dipartimento della Protezione Civile Nazionale, Milano, Italy, doi:10.13127/itaca.3.2.

Sgobba, S., G. Lanzano, F. Pacor and C. Felicetta (2021a). An Empirical Model to Account for Spectral Amplification of Pulse-Like Ground Motion Records, Geosciences, 11, 1, 15, doi:10.3390/geosciences11010015.

Sgobba, S., G. Lanzano and F. Pacor (2021b). Empirical nonergodic shaking scenarios based on spatial correlation models: An application to central Italy, Earthq. Eng. Struct. Dyn., 50, 1, 60-80, doi.org/10.1002/eqe.3362.

Spallarossa, D., G. Ferretti, P. Augliera, D. Bindi et al. (2001). Reliability of earthquake location procedures in heterogeneous areas: synthetic tests in the South Western Alps, Italy, Phys. Earth Planet. Inter., 123, 2-4, 247-266, doi:10.1016/S0031-9201(00)00213-2.

Spallarossa, D., M. Cattaneo, D. Scafidi, M. Michele et al. (2021). An automatically generated high-resolution earthquake catalogue for the 2016-2017 Central Italy seismic sequence, including P and S phase arrival times, Geophys. J. Int., 225, 1, 555-571, doi:10.1093/gji/ggaa604.

Strollo, A., D. Cambaz, J. Clinton, P. Danecek et al. (2021). EIDA: The European integrated data archive and service infrastructure within ORFEUS, Seismol. Res. Lett., 92, 3, 1788-1795, doi:10.1785/0220200413.

Sugar, C. A. (1998). Techniques for clustering and classification with applications to medical problems, PhD Dissertation, Stanford University, Department of Statistics, Stanford, XIV, 165.

Sugar, C. A., L. Lenert and R. A. Olshen (1999). An application of cluster analysis to health services research: empirically defined health states for depression from the sf-12, Technical Report, Stanford University, Stanford.

Traversa, P., E. Maufroy, F. Hollender, V. Perron et al. (2020). RESIF RAP and RLBP dataset of earthquake ground motion in mainland France, Seismol. Res. Lett., 91, 4, 2409-2424, doi.org/10.1785/0220190367.

Wells, D. L. and K. J. Coppersmith (1994). New empirical relationships among magnitude, rupture length, rupture width, rupture area, and surface displacement, Bull. Seismol. Soci. Am., 84, 4, 974-1002, doi:10.1785/BSSA0840040974.

Wilks, D. S. (2011). Statistical methods in the atmospheric sciences. Academic Press, London.

***CORRESPONDING AUTHOR: Claudia MASCANDOLA**,
Istituto Nazionale di Geofisica e Vulcanologia (INGV), Milan, Italy
e-mail: claudia.mascandola@ingv.it